molecular pharmaceutics

articles

Highly Supersaturated Solutions from Dissolution of Amorphous Itraconazole Microparticles at pH 6.8

Michal E. Matteucci,[†,‡] Joseph C. Paguio,[†] Maria A. Miller,[†] Robert O. Williams III,[§] and Keith P. Johnston*[,†]

Department of Chemical Engineering, University of Texas at Austin, Austin, Texas 78712, and College of Pharmacy, University of Texas at Austin, Austin, Texas 78712

Received July 24, 2008; Revised Manuscript Received January 5, 2009; Accepted January 8, 2009

Abstract: Dry powders from aqueous dispersions, formed by antisolvent precipitation, dissolved to form solutions with supersaturation values up to 12 in 10 min at pH 6.8 with sodium dodecyl sulfate micelles. Itraconazole/hydroxypropylmethylcellulose (HPMC) aqueous particle dispersions were salt flocculated and filtered to produce medium surface area (2−5 m^2/g) particles or lyophilized to produce high surface area (13−36 m^2/g). Over 4 h, the decay in supersaturation was much slower for the medium surface area versus high surface area particles, since the smaller excess surface area of undissolved particles led to slower nucleation and growth from solution. A slow decay in supersaturation was also achieved by initially dissolving part of the drug at pH 1.2, and then shifting the pH to 6.8 thereby reducing the excess surface area of undissolved particles in the pH 6.8 media. This pH shift mimics the transition from stomach to intestines. The ability to generate and sustain high supersaturation at pH 6.8 by minimizing undissolved excess surface area may be expected to be beneficial for raising bioavailability by gastrointestinal delivery.

Keywords: pH shift dissolution; amorphous drug; stabilization of supersaturation; surface area

1. Introduction

For poorly water soluble drugs, formulation into an amorphous form can improve the oral bioavailability by increasing the apparent solubility under physiologically relevant conditions.[1−3] Higher levels of supersaturation of the drug in the gastrointestinal tract, particularly in the upper intestine, may lead to faster permeation rates through biomembranes and thus, enhance absorption.[3−8] Solubility of amorphous drugs has been predicted to be as high as 100 to 1600 times larger than the crystalline form on the basis of thermodynamic calculations using calorimetric configu-

* To whom all correspondence should be addressed: The University of Texas at Austin, Department of Chemical Engineering, 1 University Station CO400, Austin, TX, 78712. Tel: (512) 471-4617. Fax: (512)471-7060. E-mail: kpj@che.utexas.edu.

[†] Department of Chemical Engineering.

[‡] Current address: The Dow Chemical Company, Midland, MI.

[§] College of Pharmacy.

(1) Leuner, C.; Dressman, J. Improving drug solubility for oral delivery using solid dispersions. *Eur. J. Pharm. Biopharm.* **2000**, *50*, 47–60.

(2) Hancock, B. C.; Parks, M. What is the True Solubility Advantage for Amorphous Pharmaceuticals. *Pharm. Res.* **2000**, *17* (4), 397–404.

(3) Horter, D.; Dressman, J. B. Influence of physicochemical properties on dissolution of drugs in the gastrointestinal tract. *Adv. Drug Delivery Rev.* **2001**, *46*, 75–87.

(4) Raghavan, S. L.; Trividic, A.; Davis, A. F.; Hadgraft, J. Crystallization of hydrocortisone acetate: influence of polymers. *Int. J. Pharm.* **2001**, *212* (2), 213–221.

(5) Raghavan, S. L.; Trividic, A.; Davis, A. F.; Hadgraft, J. Effect of cellulose polymers on supersaturation and in vitro membrane transport of hydrocortisone acetate. *Int. J. Pharm.* **2000**, *193* (2), 231–237.

(6) Hancock, B. C.; Zografi, G. Characteristics and significance of the amorphous state in pharmaceutical systems. *J. Pharm. Sci.* **1997**, *86*, 1–12.

(7) Kumprakob, U.; Kawakami, J.; Adachi, I. Permeation Enhancement of Ketoprofen Using a Supersaturated System with Antinucleant Polymers. *Biol. Pharm. Bull.* **2005**, *28* (9), 1684–1688.

(8) Jasti, B. R.; Berner, B.; Zhou, S.-L.; Li, X. A Novel Method for Determination of Drug Solubility in Polymeric Matrices. *J. Pharm. Sci.* **2004**, *93* (8), 2135–2141.

10.1021/mp800106a CCC: $40.75
Published on Web 02/23/2009

rational free energies.[2,9,10] However, nucleation and growth of particles from the supersaturated solution may be detrimental to absorption. Additionally, metastable amorphous and other high energy polymorphs may undergo transitions to lower energy crystalline states during the preparation and storage of the solid dosage form as well as during dissolution.[3] Consequently supersaturation levels are rarely above 10.[2,11−14] Efforts are ongoing to generate and sustain higher supersaturation levels with novel concepts in particle engineering.[15−17]

Crystallization inhibitors, such as poly(vinylpyrolidone) or hydroxypropylmethylcellulose (HPMC), have been used extensively to form amorphous solid dispersions by solvent evaporation or hot melt extrusion.[1,15−21] At loadings (drug wt/total wt) of 50% or less, the drug may be dispersed molecularly in a polymer matrix to prevent the formation of crystalline drug domains. In most cases, the relatively slow evaporation or extrusion leads to growth of particle domains on the order of 100 μm. In contrast, particle engineering by rapid precipitation upon mixing organic solutions into an antisolvent has been utilized to quench drugs into an amorphous state with surface areas up to 51 m^2/g and drug loadings up to 94%.[22,23] During precipitation, relatively small amounts of polymeric surfactants orient preferentially to the water/drug particle interface to stabilize the particles. The rapid dissolution rates of these high surface area nanoparticles limit the time for the undissolved solid phase to crystallize in the presence of the dissolution media resulting in high supersaturations in pH 1.2 media.[22] Supersaturation levels in pH 1.2 media reached 90 within 20 min, and decay of supersaturation was inhibited by arresting the growth of embryos with HPMC.[22] Similar growth inhibition was observed in an amorphous 1:1 tacrolimus/HPMC solid dispersion at pH 1.2, where a supersaturation of 25 was stable for 24 h.[17] In contrast, for a low surface area amorphous solid dispersion of a poorly water soluble drug, GWX (proprietary structure), with 60% hydroxypropyl methylcellulose phthalate (HPMCP), the solid phase crystallized within 1 min during slow dissolution that took place over 60 min resulting in a maximum supersaturation of only $\sim$3.[24]

In addition to achieving a high supersaturation, it would be desirable to target and maintain the high supersaturation in the upper intestine to increase absorption into the blood stream. Avoiding dissolution in the stomach can be advantageous since the chemical properties, such as pH, quantity of food, and residence time are variable and hard to predict.[25−27] Certain sustained release systems have been formulated for drug delivery throughout the entire GI tract to increase the

(9) Parks, G. S.; Snyder, L. J.; Cattoir, F. R. Studies on Glass. XI. Some Thermodynamic Relations of Glassy and Alpha-Crystalline Glucose. *J. Chem. Phys.* **1934**, *2*, 595–598.

(10) Gupta, P.; Chawla, G.; Bansal, A. K. Physical Stability and Solubility Advantage from Amorphous Celecoxib: The Role of Thermodynamic Quantities and Molecular Mobility. *Mol. Pharmaceutics* **2004**, *1* (6), 406–413.

(11) Mosharraf, M.; Nystrom, C. The effect of dry mixing on the apparent solubility of hydrophobic, sparingly soluble drugs. *Eur. J. Pharm. Sci.* **1999**, *9* (2), 145–156.

(12) Elamin, A. A.; Ahlneck, C.; Alderborn, G.; Nyström, N. Increased metastable solubility of milled griseofulvin, depending on the formation of a disordered surface structure. *Int. J. Pharm.* **1994**, *111*, 159–170.

(13) Corrigan, O. I.; Holohan, E. M.; Sabra, K. Amorphous forms of thiazide diuretics prepared by spray-drying. *Int. J. Pharm.* **1984**, *18* (1−2), 195–200.

(14) Stagner, W. C.; Guillory, J. K. Physical characterization of solid iopanoic acid forms. *J. Pharm. Sci.* **1979**, *68* (8), 1005–1009.

(15) Six, K.; Berghmans, H.; Leuner, C.; Cressman, J.; Van Werde, K.; Mullens, J.; Benoist, L.; Thimon, M.; Meublat, L.; Verreck, G.; Peeters, J.; Brewster, M. E.; Van den Mooter, G. Characterization of Solid Dispersions of Itraconazole and Hydroxypropylmethylcellulose Prepared by Melt Extrusion, Part II. *Pharm. Res.* **2003**, *20* (7), 1047–1054.

(16) Verreck, G.; Six, K.; Van den Mooter, G.; Baert, L.; Peeters, J.; Brewster, M. E. Characterization of solid dispersions of itraconazole and hydroxypropylmethylcellulose prepared by melt extrusion - part I. *Int. J. Pharm.* **2003**, *251*, 165–174.

(17) Yamashita, K.; Nakate, T.; Okimoto, K.; Ohike, A.; Tokunaga, Y.; Ibuki, R.; Higaki, K.; Kimura, T. Establishment of new preparation method for solid dispersion formulation of tacrolimus. *Int. J. Pharm.* **2003**, *267*, 79–91.

(18) Six, K.; Verreck, G.; Peeters, J.; Brewster, M. E.; Van den Mooter, G. Increased Physical Stability and Improved Dissolution Properties of Itraconazole, a Class II Drug, by Solid Dispersions that Combine Fast- and Slow-Dissolving Polymers. *J. Pharm. Sci.* **2004**, *93* (1), 124–131.

(19) Suzuki, H.; Sunada, H. Influence of water-soluble polymers on the dissolution of nifedipine solid dispersions with combined carriers. *Chem. Pharm. Bull.* **1998**, *46* (3), 482–487.

(20) Yamada, T.; Saito, N.; Imai, T.; Otagiri, M. Effect of grinding with hydroxypropyl cellulose on the dissolution and particle size of a poorly water-soluble drug. *Chem. Pharm. Bull.* **1999**, *47* (9), 1311–1313.

(21) Okimoto, K.; Miyake, M.; Ibuki, R.; Yasumura, M.; Ohnishi, N.; Nakai, T. Dissolution mechanism and rate of solid dispersion particles of nilvadipine with hydroxypropylmethylcellulose. *Int. J. Pharm.* **1997**, *159*, 85–93.

(22) Matteucci, M. E.; Brettmann, B. K.; Rogers, T. L.; Elder, E. J.; Williams, R. O., III; Johnston, K. P. Design of Potent Amorphous Drug Nanoparticles for Rapid Generation of Highly Supersaturated Media. *Mol. Pharmaceutics* **2007**, *4* (5), 782–793.

(23) Muhrer, G.; Meier, U.; Fusaro, F.; Albano, S.; Mazzotti, M. Use of compressed gas precipitation to enhance the dissolution behavior of a poorly water-soluble drug: Generation of drug microparticles and drug-polymer solid dispersions. *Int. J. Pharm.* **2006**, *308*, 69–83.

(24) Sertsou, G.; Butler, J.; Hempenstall, J.; Rades, T. Solvent change co-precipitation with hydroxylpropyl methylcellulose phthalate to improve dissolution characteristics of a poorly water-soluble drug. *J. Pharm. Pharmacol.* **2002**, *54*, 1041–1047.

(25) Honkanen, O.; Marvola, J.; Kanerva, H.; Lindevall, K.; Lipponen, M.; Kekki, T.; Ahonen, A.; Marvola, M. Gamma scintigraphic evaluation of the fate of hydroxypropyl methylcellulose capsules in the human gastrointestinal tract. *Eur. J. Pharm. Sci.* **2004**, *21*, 671–678.

(26) Kararli, T. T. Comparison of the gastrointestinal anatomy, physiology, and biochemistry of humans and commonly used laboratory animals. *Biopharm. Drug Dispos.* **1995**, *16* (5), 351–380.

(27) Mojaverian, P. Evaluation of Gastrointestinal pH and Gastric Residence Time via the Heidelberg Radiotelemetry Capsule: Pharmaceutical Application. *Drug Dev. Res.* **1996**, *38*, 73–85.

therapeutic window of crystalline and amorphous poorly water soluble drugs.[28−31] Enteric or sustained drug release can be achieved with pH sensitive polymers such as methacrylic acid/methylmethacrylate copolymers, for example Eudragits[32,33] or HPMCP [24,34−36] or with pH sensitive hydrogels. [37,38] However, *in vitro* supersaturation curves at pH values above about 6 are rarely reported. Furthermore, most previous studies of supersaturation only considered low surface area (<1 m^2/g) morphologies, with particles larger than about 5 μm.

The method of drying an aqueous particle suspension can have a large effect on the particle size, crystallinity and thus the resulting dissolution behavior. Recently, we reported that itraconazole (ITZ) nanoparticles (300 nm) coated with a nonionic polymeric stabilizer may be recovered from an aqueous dispersion by flocculation with a divalent salt.[39,40] The micron-sized flocs could then be filtered (1−3 μm pore size) and dried to obtain a powder. The dried powders redispersed in water to their original particle size.[40] This method provides rapid recovery of nanoparticles with minimal residual water evaporated, and increased drug loading since the free stabilizer is removed during filtration. Although high supersaturation levels of ∼14 were achieved in pH 6.8 media for these high surface area particles, the rapid decay in supersaturation resulted in a supersaturation of only ∼4.5 after 1 h.[39] In the current work, we vary the polymeric stabilizer in this salt flocculation technique to achieve greater control of the particle size.

The objective of this study was to design ITZ particles ranging in size from 200 nm to 45 μm and examine how well supersaturation levels are maintained upon dissolution of these particles in pH 6.8 media with SDS micelles. To probe supersaturation mechanisms, the behavior of particles with high (>10 m^2/g, nanoparticles) and medium (2−5 m^2/g, microparticles) surface areas is compared to more commonly studied particles with low (<2 m^2/g) surface area. High surface area particles facilitate rapid dissolution rates of poorly water soluble crystalline[41−43] and amorphous[1−3] drugs. However, the high surface area of the dissolving particles may cause depletion in the level of supersaturation[39] by accelerating heterogeneous nucleation, as well as growth by condensation and coagulation. Thus, we propose that medium surface areas may be optimal for balancing two competing effects: (1) sufficient dissolution rate to avoid solvent-mediated crystallization of the undissolved solid phase and (2) minimization of heterogeneous sites for nucleation and growth of particles from the supersaturated solution.

Medium surface area particles were produced by salt flocculation of aqueous dispersions of ITZ particles stabilized by HPMC, whereby the controlled growth of drug domains during flocculation led to the appropriate size. High surface area particles were produced by antisolvent precipitation (AP) with the stabilizers EudragitL100 and HPMC. The contrasting low surface area solid dispersion particles were produced by solvent evaporation. The resulting effect of undissolved

(28) Gan, Y.; Pan, W.; Wei, M.; Zhang, R. Cyclodextrin complex osmotic tablet for glipizide delivery. *Drug Dev. Ind. Pharm.* **2002**, *28*, 1015–1021.

(29) Liu, L.; Khang, G.; Rhee, J. M.; Lee, H. B. Monolithis osmotic tablet system for nifedipine delivery. *J. Controlled Release* **2000**, *67*, 309–322.

(30) Yang, M. S.; Cui, F. D.; You, B. G.; Fan, Y. L.; Wang, L.; Yue, P.; Yang, H. Preparation of sustained-release nitrendipine microspheres with Eudragit RS and Aerosil using quasi-emulsion solvent diffusion method. *Int. J. Pharm.* **2003**, *259*, 103–113.

(31) Yang, M.; Cui, F.; You, B.; You, J.; Wang, L.; Zhang, L.; Kawashima, Y. A novel pH-dependent gradient-release delivery system for nitrendipine I. Manufacturing, evaluation in vitro and bioavailability in healthy dogs. *J. Controlled Release* **2004**, *98*, 219–229.

(32) De Jaeghere, F.; Allemann, E.; Kubel, F.; Galli, B.; Cozens, R.; Doelker, E.; Gurny, R. Oral bioavailability of a poorly water soluble HIV-1 protease inhibitor incorporated into pH-sensitive particles: effect of the particle size and nutritional state. *J. Controlled Release* **2000**, *68*, 291–298.

(33) Debunne, A.; Vervaet, C.; Remon, J.-P. Development and in vitro evaluation of an enteric-coated multiparticulate drug delivery systems for the administration of piroxicam to dogs. *Eur. J. Pharm. Biopharm.* **2002**, *54* (3), 343–348.

(34) Hasegawa, A.; Taguchi, M.; Suzuki, R.; Miyata, T.; Nakagawa, H.; Sugimoto, I. Supersaturation Mechanism of Drugs from Solid Dispersions with Enteric Coating Agents. *Chem. Pharm. Bull.* **1988**, *36* (12), 4941–4950.

(35) Tanno, F.; Nishiyama, Y.; Kokubo, H.; Obara, S. Evaluation of Hypromellose Acetate Succinate (HPMCAS) as a Carrier in Solid Dispersions. *Drug Dev. Ind. Pharm.* **2004**, *30* (1), 9–17.

(36) Kohri, N.; Yamayoshi, Y.; Xin, H.; Iseki, K.; Sato, N.; Todo, S.; Miyazaki, K. Improving the oral bioavailability of albendazole in rabbits by the solid dispersion technique. *J. Pharm. Pharmacol.* **1999**, *51* (2), 159–164.

(37) Scott, R. A.; Peppas, N. A. Highly crosslinked, PEG-containing copolymers for sustained solute delivery. *Biomaterials* **1999**, *20* (15), 1371–1380.

(38) Fukuda, M.; Peppas, N. A.; McGinity, J. W. Properties of sustained release hot-melt extruded tablets containing chitosan and xanthan gum. *Int. J. Pharm.* **2006**, *310* (1−2), 90–100.

(39) Matteucci, M. E.; Paguio, J. C.; Mazuski, M. A.; Williams III, R. O.; Johnston, K. P. Flocculated Amorphous Nanoparticles for Highly Supersaturated Solutions. *Pharm. Res.* **2008**, *25* (11), 2477–2487.

(40) Chen, X. Nanoparticle Engineering Processes: Evaporative Precipitation into Aqueous Solution (EPAS) and Antisolvent Precipitation to Enhance the Dissolution Rates of Poorly Water Soluble Drugs. PhD. Dissertation, University of Texas, Austin, 2004.

(41) Gassman, P.; List, M.; Schweitzer, A.; Sucker, H. Hydrosols-Alternatives for the parenteral application of poorly water-soluble drugs. *Eur. J. Pharm. Biopharm.* **1994**, *40* (2), 64–72.

(42) Liversidge, E. M.; Liversidge, G. G.; Cooper, E. R. Nanosizing: a formulation approach for poorly-water-soluble compounds. *Eur. J. Pharm. Sci.* **2003**, *18*, 113–120.

(43) Muller, R. H.; Bohm, B. H. L. Nanosuspensions. In *Emulsions and Nanosuspensions for the Formulation of Poorly Soluble Drugs*; Muller, R. H., Benita, S., Bohm, B. H. L., Eds.; Medpharm Scientific: Stuttgart, 1998; pp149−174.

(44) Crisp, M. T.; Tucker, C. J.; Rogers, T. L.; Williams, R. O., III; Johnston, K. P. Turbidimetric measurement and prediction of dissolution rates of poorly soluble drug nanocrystals. *J. Controlled Release* **2007**, *117*, 351–359.

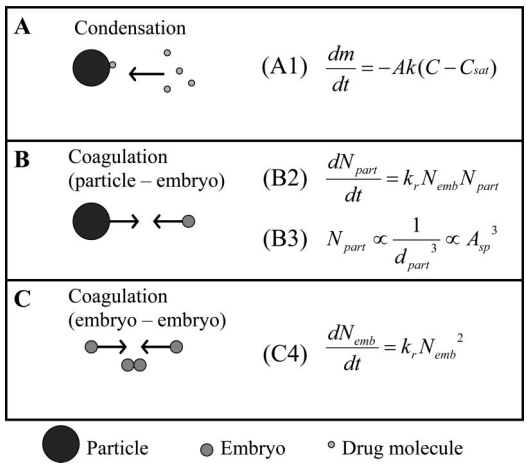

Figure 1. Mechanisms for depletion of supersaturation, where m is mass of drug in solution, A is the total particle surface area, C is the drug solution concentration, C_{sat} is the drug solubility, N_{part} is the number of drug particles per volume, k_r is a rate constant, N_{emb} is the number of embryos per volume, A_{sp} is the specific surface area (area/mass), and d_{part} is the diameter of the particle.

particles on nucleation and growth from supersaturated solution is compared for the various particle surface areas. Whereas most experiments were performed exclusively at pH 6.8, in one case the pH was shifted from 1.2 to pH 6.8 after 2 h to mimic the transition from the stomach to upper intestine.

2. Theory of Nucleation and Growth from Supersaturated Solution

Amorphous particles may dissolve to form metastable highly supersaturated solutions. Particles may precipitate from these metastable solutions to lower the free energy depending upon the rate of nucleation to form particle embryos followed by growth via condensation (Figure 1A) or coagulation (Figure 1B,C). The growing particles may crystallize to form a less soluble form than the amorphous polymorph.[2] Homogeneous nucleation is highly sensitive to the degree of supersaturation S as follows[45]

$$B_o = C \exp\left(\frac{-16\pi\gamma^3 V_m^2 N_A}{3(RT)^3(\ln(S))^2}\right) \quad (1)$$

where C is the frequency factor, γ is the interfacial tension, V_m is the molar volume of the solute, and N_A is Avogadro's number. The nucleation and growth competes with dissolution of the original amorphous particles. In addition, the original undissolved particles may crystallize when exposed to the solvent also lowering the achievable supersaturation.[11] Condensation of dissolved molecules onto these crystals will also deplete supersaturation. The rate of growth by condensation is directly proportional to excess surface area, defined as the surface area of undissolved particles, according to eq A1 from Figure 1.[46] Therefore, the condensation rate may be much faster for the very small initial particles with high excess surface area. Growth by coagulation (Figure 1B,C) is dependent on N_{part}^2 where N_{part} is the number of particles for a given stability ratio.[47] For a constant mass of drug, N_{part} is proportional to the particle diameter, d_{part}^{-3}, and specific surface area, A_{sp}^3 (Figure 1, eq B3). For example, a 10-fold increase in d_{part} decreases the specific surface area by a factor of 10 and the coagulation rate by a factor of 10^3 (Figure 1, eq B2).[47]

3. Materials and Methods

3.1. Materials. B.P. grade itraconazole (ITZ) was purchased from Hawkins, Inc. (Minneapolis, MN). HPMC E5 (viscosity of 5 cP at 2% aqueous 25 °C solution) grade was a gift from The Dow Chemical Corporation. Methacrylic acid−methylmethacrylate copolymer (1:1 ratio), Eudragit L100 (EL100) was donated by Degussa Röhm America LLC (Piscataway, NJ). Stabilized p.a. grade 1,3-dioxolane was obtained from Acros Organics (Morris Plains, NJ). HPLC grade acetonitrile (ACN), ACS grade hydrochloric acid (HCl), diethanolamine (DEA), sodium dodecyl sulfate (SDS), sodium sulfate anhydrous (Na_2SO_4), and ACS certified tribasic sodium phosphate (Na_3PO_4) were used as received from Fisher Chemicals (Fairlawn, NJ).

3.2. Experimental Details. 3.2.1. Antisolvent Precipitation (AP) into Aqueous Solution. The method of antisolvent precipitation was used to produce nanoparticle suspensions of ITZ.[48] For HPMC-stabilized particles, deionized water (50 g) containing an appropriate quantity of HPMC was used as the antisolvent phase into which 15 g of 1,3-dioxolane containing 3.3% (wt) ITZ was injected using a 19G syringe and a flow rate of ~300 mL/min to form a fine precipitate. The organic phase was separated from the aqueous suspension via vacuum distillation. The aqueous suspension was then added dropwise to liquid nitrogen and lyophilized to form a powder using a Virtis Advantage Tray Lyophilizer (Virtis Company, Gardiner, NY) with 24 h of primary drying at −35 °C followed by 36 h of secondary drying at 25 °C. ITZ/HPMC particle dispersions were also salt flocculated and rapidly filtered, as described by a previous study.[40] Briefly, 120 mL of 1.5 M Na_2SO_4 was added to 50 mL of aqueous suspension to form loose flocculates which could be rapidly filtered in ~10 min. The filter cake was dried at ambient conditions for at least 12 h.

(45) McCabe, W. L.; Smith, J. C.; Harriott, P. *Unit Operations of Chemical Engineering*, 6th ed.; McGraw-Hill: New York, 2001.

(46) Mullin, J. W. *Crystallization*, 3rd ed.; Butterworth-Heinemann: Boston, 1997.

(47) Heimenz, P. C.; Rajagopalan, R. *Principles of Colloid and Surface Chemistry*, 3rd ed.; Marcel Dekker, Inc.: New York, 1997.

(48) Rogers, T. L.; Gillespie, I. B.; Hitt, J. E.; Fransen, K. L.; Crowl, C. A.; Tucker, C. J.; Kupperblatt, G. B.; Becker, J. N.; Wilson, D. L.; Todd, C.; Broomall, C. F.; Evans, J. C.; Elder, E. J. Development and Characterization of a Scalable Controlled Precipitation Process to Enhance the Dissolution of Poorly Water-Soluble Drugs. *Pharm. Res.* **2004**, *21* (11), 2048–2057.

For EL100-stabilized particles, 3.1 g of 4% EL100 in methanol was added to 15 g of 3.3% (wt) ITZ solution in 1,3-dioxolane to achieve a 4:1 ratio of ITZ to EL100. The ITZ/EL100 organic solution was then injected into 100 mL of 10^{-4} N HCl (pH 3.3) to form a coprecipitate. Alternatively, 6.2 g of 2% EL100 in methanol was added dropwise to 100 mL of pure water to form a clear solution. Into the aqueous EL100 solution, 15 g of 3.33% ITZ solution in 1,3-dioxolane was injected to form a fine precipitate at the 4:1 ratio of ITZ to EL100. After the organic solvents were removed, the suspensions were freeze-dried as described above.

3.2.2. Solvent Evaporation To Form a Solid Dispersion (SD). Approximately 2 g of ITZ was added to 20 mL of dichloromethane and agitated until completely dissolved. The ITZ solution was placed in a mortar, and 1 g of HPMC was slowly added while gently stirring with a pestle without any precipitation. The solution was stirred gently until approximately 90% of the dichloromethane volume was evaporated, leaving a clear viscous gel. The remaining dichloromethane was removed by heating to 50 °C at a reduced pressure of ~500 mTorr for 2 h. The resulting drug/polymer film was removed from the mortar and pestle with a straight razor blade and ground to a fine powder for 30 min using a ceramic ball mill (1 cm bead size). The final powder was collected after filtration through a size 16 mesh sieve (<1190 μm pore size).

3.2.3. Solubility Determination. To determine the solubility of crystalline ITZ at 37.2 °C, approximately 1.5 mg of bulk ITZ was placed in a glass vials containing 100 mL of pH 6.8 media with 0.17% SDS wt/vol. The medium was made by adding 0.2 M tribasic sodium phosphate to 0.1 N HCl at a volume ratio of 1:3, followed by addition of 0.17% SDS. When necessary, the pH was adjusted to 6.8 by addition of 1 N HCl. Two aliquots were removed from each vial after 18 h and 24 h, immediately filtered with a 0.2 μm syringe filter and diluted with ACN to double the volume. Drug concentration was determined by high performance liquid chromatography as described below with at least an $n = 3$.

3.2.4. Dissolution under Supersaturated Conditions. Rates of supersaturation were measured in pH 6.8 medium (as described above) with 0.17% SDS at 37.2 °C. A USP paddle method was adapted to accommodate small sample sizes using a VanKel VK6010 Dissolution Tester with a Vanderkamp VK650A heater/circulator (VanKel, Cary, NC). Dissolution medium (50 mL) was preheated in small 100 mL capacity dissolution vessels (Varian Inc., Cary, NC). Dry powder (~17.6 mg drug) equivalent to approximately 25 times the equilibrium solubility of ITZ in pH 6.8 buffer with SDS ($C_{eq} = 14$ μg/mL, from solubility study) was added to the medium at time zero. In some cases, a smaller dose was added equivalent to 15 times the equilibrium solubility (10.5 mg ITZ) or 5 times the equilibrium solubility (3.5 mg ITZ). For all neutral pH media dissolution experiments, 1.0 mL aliquots were taken after 10, 20, 30, 60, 120, and 240 min. For the pH shift experiment, dry powder (~17.6 mg drug) was added to 60 mL of 0.1 N HCl and 1.0 mL aliquots were taken at 10, 20, 30, 60, and 120 min. After 120 min, 20 mL of 0.2 M tribasic sodium phosphate with 0.68% SDS was added to shift the pH to 6.8 with a final concentration of 0.17% SDS. Sample aliquots (1.0 mL) were taken at 10, 20, 30, 60, and 120 min after the pH shift. For all dissolution experiments, the aliquots were filtered immediately using a 0.2 μm syringe filter and 0.8 mL of the filtrate was subsequently diluted with 0.8 mL of ACN. In all cases, the filtrate was completely clear upon visual inspection and dynamic light scattering of the filtrate gave a count rate of less than 20K cps (too small for particle size analysis). The drug concentration was quantified by high performance liquid chromatography as described below.

3.2.5. High Performance Liquid Chromatography (HPLC). ITZ concentrations were quantified using a Shimadzu LC-600 HPLC (Columbia, MD). The mobile phase was ACN:water:DEA 70:30:0.05, and the flow rate was 1 mL/min. For a detection wavelength of 263 nm, the ITZ peak elution time was 5.4 min. The standard curve linearity was verified from 1 to 500 μg/mL with an r^2 value of at least 0.999.

3.2.6. Scanning Electron Microscopy (SEM). Dry powder samples were placed on adhesive carbon tape and gold−palladium sputter coated for 45 s. Micrographs were taken using a Hitachi S-4500 field emission scanning electron microscope with an accelerating voltage of 15 kV.

3.2.7. Temperature Modulated Differential Scanning Calorimetry (DSC). Drug crystallinity was detected by a 2920 modulated DSC (TA Instruments, New Castle, DE) with a refrigerated cooling system. Samples were placed in hermetically sealed aluminum pans and purged with nitrogen at a flow rate of 150 mL/min. The amplitude used was 1 °C, the period 1 min, and the underlying heating rate 5 °C/min. Integration under the recrystallization peak around 120 °C (Δh_{cryst}) and the melting endotherm around 168 °C (Δh_{melt}) were used to estimate the percent crystallinity in the original samples by

$$\%\text{cryst} = \frac{\Delta h_{melt} - \Delta h_{cryst}}{\Delta h_{meltITZ}} \quad (2)$$

where $\Delta h_{meltITZ}$ is the heat of melting for pure crystalline ITZ. This assumes that the heat necessary to melt 1 g of crystalline ITZ and the heat necessary to melt an equal amount of amorphous ITZ are equal.

3.2.8. BET Surface Area Measurement. Powder specific surface areas of drug powder were measured using a Quantichrome Instruments Nova 2000 series surface area analyzer (Boynton Beach, FL) using nitrogen as the adsorbate gas. Six points were taken over a range of relative pressures from 0.05 to 0.35. In all cases, correlation coefficients were greater than 0.99, indicating good linear fit with the Brunauer−Emmett−Teller (BET) equation.

3.2.9. Particle Size Analysis. Particle size distributions were measured by multiangle laser light scattering using a Malvern Mastersizer-S (Malvern Instruments Inc., Southborough, MA). For measurements of the particle dispersion, approximately 5 mL of suspension was diluted with 500 mL of pure deionized water to obtain an obscuration between

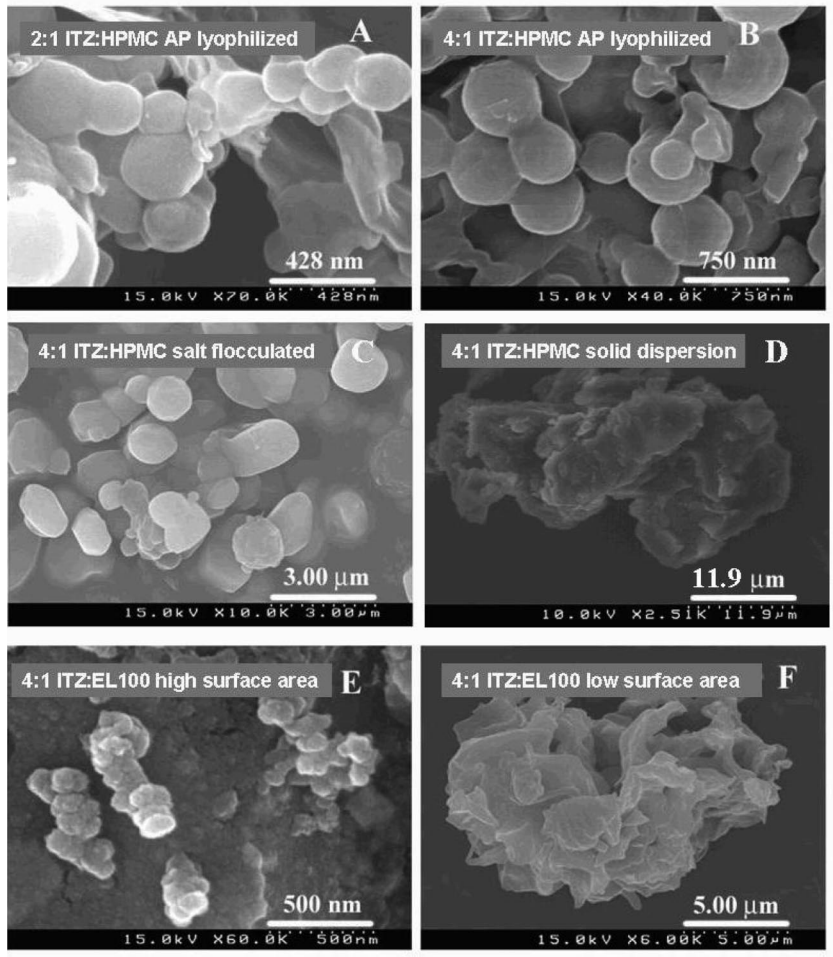

Figure 2. Scanning electron microscopy images of various ITZ particles stabilized by HPMC or EL100 produced by antisolvent precipitation or a solvent evaporation solid dispersion technique.

10% and 20%. For measurements of dried particles, approximately 0.1 g of the dried particles was added to 20 mL of DI water and sonicated for 1 min using a Branson Sonifier 450 (Branson Ultrasonics Corporation, Danbury, CT) with a 102 converter and tip operated in pulse mode at 35 W. Distributions, based on volume fraction, were calculated with a refractive index of 1.610 for itraconazole.

4. Results and Discussion

4.1. Particle Engineering To Control Surface Area and Morphology. As shown in Figure 2 and BET results from Table 1, a range of particle sizes was produced by AP and solvent evaporation. The flash frozen and lyophilized AP 2:1 and 4:1 ITZ/HPMC dispersions were composed of primary particles approximately 200−500 nm in diameter, according to SEM (Figure 2A,B), and with a high specific surface area (13−17 m^2/g from BET), as reported previously.[22] According to static light scattering, the primary particles of the original 4:1 ITZ/HPMC AP dispersion formed ~3 μm aggregates. For the flash-frozen lyophilized particles, static light scattering measurements also indicated that the 500 nm primary particles shown by SEM (Figure 2A,B) formed aggregates of 2−5 μm upon redispersion in water.

AP nanoparticle aggregates were also recovered by flocculation with salt and filtration. The salt desolvates the polymeric stabilizers, resulting in strong attractive forces between particles and rapid flocculation to form microparticles on the order of 50 μm, which may be filtered easily.[40] After drying, the salt flocculated particles were redispersed in water to form 10 μm aggregates as characterized by static light scattering. In this case, the primary domains of the salt flocculated aggregates were 2−3 μm in diameter, according to SEM (Figure 2C). Therefore, some particle growth occurred during the salt flocculation/filtration process, as the primary domains increased from ~500 nm to ~3 μm. BET surface area measurements (Table 1) were in good agreement with the primary particle size observed by SEM, as the value decreased from 13 to 4.4 m^2/g for lyophilized and salt flocculated 4:1 ITZ/HPMC, respectively.

In a previous study, 300 nm primary particles of ITZ stabilized by HPMC and poly(ethylene oxide-*b*-propylene oxide-*b*-ethylene oxide) (poloxamer 407) were formed by AP without any aggregation, as observed by static light scattering. The poloxamer 407 provided additional stabilization, as the primary particles in these dispersions did not undergo growth when flocculated by salt and filtered ac-

Table 1. BET Surface Areas, AUCs, Surface Area from Excess Particles during Dissolution and Supersaturation Depletion Rates from Supersaturation Dissolution Studies at pH 6.8

dissolution in pH 6.8	dose (μg/mL)/ (14 μg/mL)	surface area (m^2/g)	pH 6.8 AUC_{4h} (min)	excess surface area (m^2)	max supersaturation (in pH 6.8)	supersaturation depletion rate (min^{-1})
2:1 ITZ/HPMC Lyo	25	17	765	0.12	16	1.0
2:1 ITZ/HPMC Lyo	15	17	1072	0.036	13	0.17
2:1 ITZ/HPMC Lyo	5	17	843	0.012	4	negligible
2:1 ITZ/HPMC Lyo	incremental	17	1602	~0	8	negligible
4:1 ITZ/HPMC Lyo	25	13	845	0.11	12	0.38
4:1 ITZ/HPMC salt	25	4.4	1869	0.04	14	0.10
4:1 ITZ/HPMC SD	25	<1[a]	388	<0.01	2.8	
4:1 ITZ/EL100						
high surface area	25	35	1154	0.32	12	0.22
low surface area	25	1.2	1210	0.021	6.5	negligible
dissolution with pH shift			pH 6.8 AUC_{2h}			
Sporanox	25	–	403			
4:1 ITZ/HPMC Lyo	25	13	939	0.14	12.5	0.022

[a] Specific surface area based on lower detection limit of BET surface area analyzer.

cording to SEM.[39] In addition, when the particles were added to water, static light scattering measurements showed that they redispersed back to their original size of 300 nm indicating the flocculation was reversible. Comparing these previous results for the HPMC and poloxamer 407 stabilized particles[39] with those for only HPMC in this study, demonstrates that the particle size and surface area may be tuned in the salt flocculation process by varying the composition of the stabilizers.

For the AP process, the solubility of polymeric stabilizer in the aqueous phase was varied to manipulate the particle size. To form high surface area nanoparticles, the stabilizer must adsorb to drug particles and be solvated by water to arrest growth.[49] This behavior was achieved for HPMC in water or EL100 in a water/methanol mixture, as seen in Figure 2A,B,E with primary particles on the order of 200−500 nm. When the aqueous phase was changed to a 10^{-4} N HCl solution (pH 3.3) without methanol, the acrylic acid groups of EL100 were protonated, rendering the polymer insoluble, leading to limited diffusion and adsorption of polymer to the drug surfaces, giving a low surface area of 1.2 m^2/g (Table 1, Figure 2F). The control of the particle size by varying polymer solvation has received limited attention in antisolvent precipitation with water soluble stabilizers such as HPMC,[22] polyvinylpyrolidone,[40,48] and poloxamer 407.[40,48,49] Therefore, the ability to tune the solubility of pH dependent polymers such as EL100 is a key advantage for controlling the particle surface area over a wide range. For comparison, very large ~45 μm SD particles were produced by solvent evaporation with a surface area <1 m^2/g (Figure 2D).

The morphology of particles produced by AP and solvent evaporation was investigated by DSC, as shown in Figure 3, with arrows to indicate crystallization and melting events. The melting temperature of bulk pure ITZ was 168 °C (curve I). In curves B−D, the first slight transition viewed at ~60 °C is the glass transition temperature of ITZ[15] followed by the crystallization of amorphous ITZ that was seen upon heating at 115−125 °C. Since the area of the melting peak was slightly larger than that of the crystallization peak, these formulations were mostly amorphous below the crystallization temperature ~115 °C. In the case of 2:1 ITZ/HPMC AP lyophilized (curve A in Figure 3) and the high and low surface area 4:1 ITZ/EL100 (curves E and F in Figure 3), the crystallization peak was small and when coupled with a small melting peak area for ITZ, indicate that these formulations have even more stable amorphous behavior than the other formulations. The 2:1 ITZ/HPMC AP lyophilized sample (curve A) is expected to be more stable due to the increase in stabilizing polymer in the sample.[22] However, maintaining the amorphous nature of the EL100 samples, even at high temperatures where crystallization can be seen in many high potency samples, can be attributed the more specific binding stability between ITZ and EL100 due to the Lewis acid binding sites on ITZ and negatively charged acrylic acid groups of the EL100.[50]

Metastable amorphous ITZ may be produced by the rapid AP process followed by lyophilization (Figure 3 curves A, B, E, and F), even at drug loadings of 80% (drug wt/total wt), as reported previously for HPMC stabilized samples (Figure 3 curves A, B)[22] and currently for EL100 stabilized samples (Figure 3 curves E, F). In these cases, the metastable amorphous state was quenched before drug domains crystallized. This behavior has also been achieved even without any stabilizer present.[22] As is evident in curve C of Figure

(49) Matteucci, M. E.; Hotze, M. A.; Williams, R. O., III; Johnston, K. P. Drug Nanoparticles by Antisolvent Precipitation: Mixing Energy Versus Surfactant Stabilization. *Langmuir* **2006**, *22* (21), 8951–8959.

(50) Miller, D. A.; DiNunzio, J. C.; Yang, W.; McGinity, J. W.; Williams, R. O., III. Targeted Intestinal Delivery of Supersaturated Itraconazole for Improved Oral Absorption. *Pharm. Res.* **2008**, *25* (6), 1450–1459.

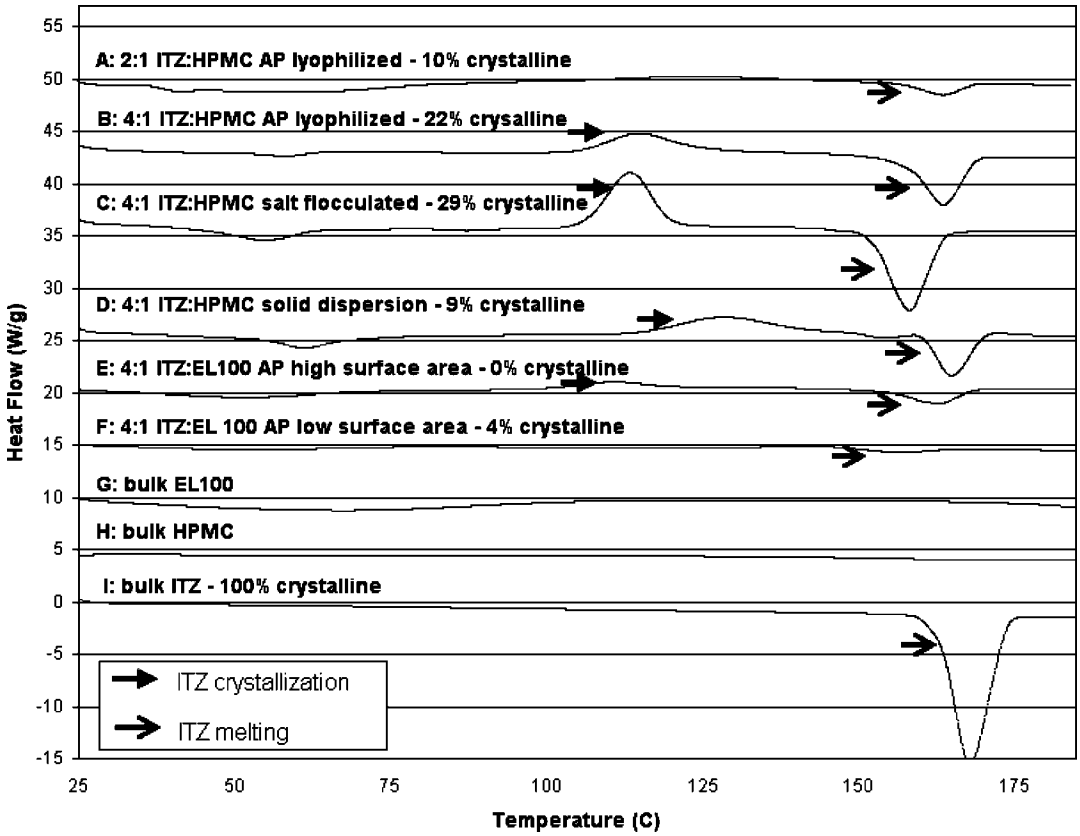

Figure 3. Differential scanning calorimetry of various ITZ particles and the bulk components. % crystallinity values of each engineered formulation are calculated using eq 2.

3, AP nanoparticles remain mostly amorphous throughout the salt flocculation process, even at the same high drug loading of 80%. The salt flocculation was conducted at ~25 °C, well below the glass transition temperature of ITZ (58 °C[15]), to minimize mobility of the drug molecules and mitigate crystallization. While the amorphous morphology is preserved as nanoparticles are flocculated to form medium surface area particles during the salt flocculation process, the significantly higher temperatures in spray drying often produced crystallization of amorphous nanoparticles.[39]

4.2. Generation of Supersaturation from Particle Dissolution. The dissolution rate was compared for ITZ particles as a function of surface area to investigate the rate of generation of supersaturation at short times. The complete behavior will be explained more fully in the next section, which will also consider the loss of supersaturation to nucleation and growth from solution. As shown in Figures 4 and 5, both the high and medium surface area particles dissolved rapidly to give supersaturation values of approximately 12 in less than 20 min. The peak supersaturation reached 14 for the medium surface area 4:1 ITZ/HPMC salt flocculated AP particles, much higher than typical values of 6 (based on C_{eq} of ~10 μg/mL) for SD particles in pH 6.8 buffer.[24,34,35] Low surface area 4:1 ITZ/EL100 slowly dissolved to a supersaturation of 6 after 2 h, as shown in Figure 5, while low surface area 4:1 ITZ/HPMC SD particles only reached a maximum supersaturation level of 2.9 in 30 min (Figure 4).

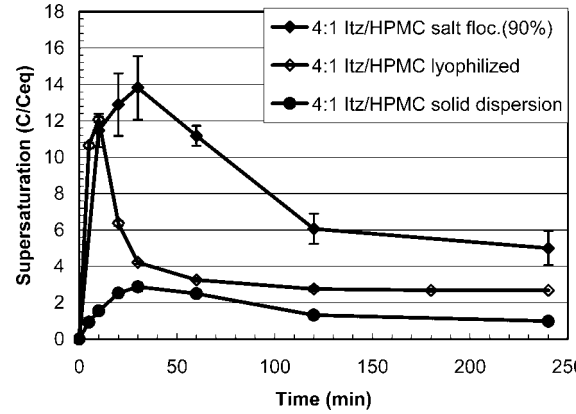

Figure 4. Supersaturation in pH 6.8 buffer with 0.17% SDS from dissolution of ITZ/HPMC particles at a dose of 25 (17.5 mg of ITZ added to 50 mL).

Rapid dissolution shortens the time for crystallization of undissolved particles in the presence of the dissolution media, offering the potential to increase the maximum supersaturation. As seen in Figures 4 and 5 and in our previous studies,[22,51] the design of more rapidly dissolving amorphous particles (high and medium surface area particles) has the potential to raise maximum supersaturation values markedly relative to more conventional low surface area solid dispersions. The theoretical supersaturation, calculated using configurational thermodynamics, is between 95 and 125 at a temperature of 37 °C for pure ITZ,[51] however the experimentally achievable magnitude of supersaturation is

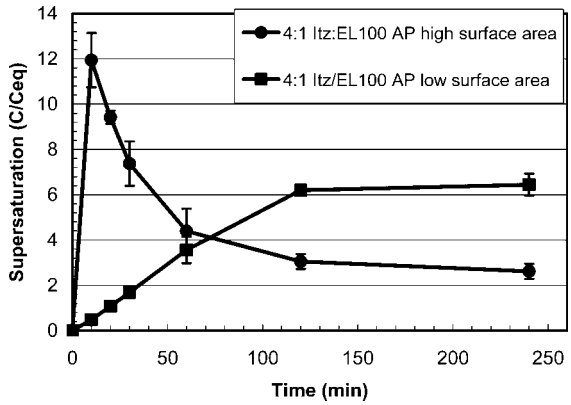

Figure 5. Supersaturation in pH 6.8 with 0.17% SDS from dissolution of low and high surface area 4:1 ITZ/EL100 AP particles at a dose of 25.

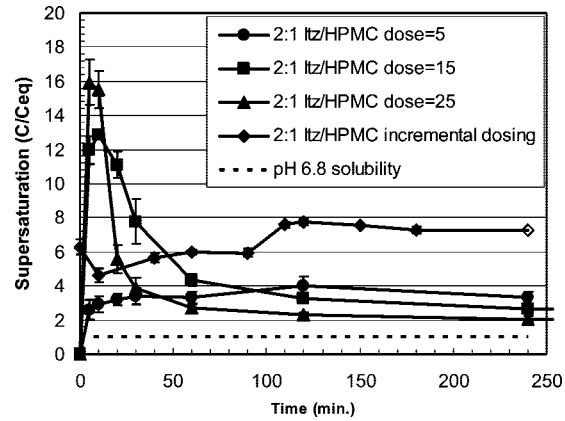

Figure 6. Supersaturation in pH 6.8 buffer with 0.17% SDS from dissolution of 2:1 ITZ/HPMC AP lyophilized particles at doses of 5, 15, 25, and incremental addition to 8.

dependent on the media used for the study as well as the partial crystallinity and wettability of the solution.[51] Previously, pure dissolution studies in pH 1.2 media demonstrated supersaturations up to 90.[22,51] However, the medium used here, pH 6.8 with 0.17% SDS, more closely relates to the pH in the intestines with added SDS micelles to increase the solubility of ITZ. As a result, the highest measured supersaturation in this micellar medium is approximately 16 (Table 1).

The overall dissolution rate of a drug particle in a micellar solution is governed by both the uptake of the drug molecules by the micelle as well as the diffusion of the loaded micelle away from the drug particle.[44] Since these two steps can be combined to give an overall effective rate constant k_{eff}, the dissolution into a micellar solution can be modeled as

$$\frac{\mathrm{d}m}{\mathrm{d}t} = k_{\text{eff}} A C_{\text{sat}} \tag{3}$$

where A is the specific surface area. As a result, increasing the specific surface area of the drug particles by decreasing the particle size creates a faster dissolution rate and creating the potential to achieve higher supersaturation.

4.3. Depletion of Supersaturation via Nucleation and Growth on Undissolved Particles. 4.3.1. Effect of Dose and Excess Surface Area. The effect of nucleation and growth on the undissolved particles was first measured by varying the dose of particles added to the dissolution media to manipulate the excess surface area of undissolved particles. As shown in Figure 1 and discussed in the theory section, an increase in excess surface area may accelerate the rate of depletion of the supersaturation by enhancing nucleation and growth rates. The excess surface area after 10 min of dissolution at pH 6.8 was calculated by

$$\text{excess SA} = (\text{particle SA})[S_{\text{T}} - S_{\text{D}}] \tag{4}$$

where particleSA is the particle specific surface area measured by BET, S_{T} is the total dose added and S_{D} is the total amount dissolved after 10 min.

For high surface area lyophilized 2:1 ITZ/HPMC, the dose was varied from 25 to 5 (Figure 6 and Table 1). The excess surface areas corresponding to doses of 25, 15, and 5 were 0.12, 0.036, and 0.012 m^2 respectively (corresponding to the supersaturation after 10 min in each case). The rate of depletion in supersaturation was estimated by taking the initial slope of the depletion phase in supersaturation curves, starting at the maximum in drug concentration. At the lowest dose of 5, the supersaturation of only 4 produced a relatively small driving force for nucleation (eq 1) and growth (Figure 1, eq A1) and thus decay in supersaturation over the 4 h experiment. At a higher dose of 15, the supersaturation reached a much higher level of 13, resulting in a much faster depletion rate of $\sim$0.17 min^{-1} due to a larger driving force for faster nucleation (eq 1) and a three times higher excess surface area of undissolved particles producing faster growth rates by condensation and coagulation (Figure 1). Finally, the highest supersaturation and depletion rates were observed for the largest dose of 25, continuing the trends seen for the increase in dose.

In a control experiment, high surface area 2:1 ITZ/HPMC powder was added incrementally, in small doses to avoid building up excess surface area. An initial dose of 5 mg dissolved completely with a linear slope over 1 h (results not shown). An additional dose of 2 mg was added after 1 h and again after 90 min (profile shown in Figure 6) for a total dose of 9 mg in 80 mL. All of the added particles dissolved, as indicated by the supersaturation level of 8 (112 μg/mL, the total added dose), for an excess surface area of essentially 0. In another control experiment, undissolved particles from a highly supersaturated solution ($\sim$15$\times$) were removed after 10 min of dissolution by filtration with a 0.2 μm syringe filter to attempt to minimize decay in the supersaturation. HPLC analysis verified that a supersaturation of 12.5 was sustained for 30 min without any precipitation (results not shown). In each of these control experiments, supersaturation

(51) Matteucci, M. E.; Miller, M. A.; Williams, R. O., III; Johnston, K. P., Highly Supersaturated Solutions of Amorphous Drugs Approaching Predictions from Configurational Thermodynamic Properties. *J. Phys. Chem. B*, in press.

levels did not decay when excess particles were absent. Homogeneous nucleation rates appeared to be too slow to deplete the supersaturation levels of 8−12. Therefore, depletion rates of supersaturation are much slower in media where excess surface area from undissolved particles is minimized.

4.3.2. High Surface Area Particles. At a constant dose of 25, high surface area lyophilized 4:1 and 2:1 ITZ/HPMC rapidly dissolved to a supersaturation of 12−16, followed by depletion to ~3 within 1 h, as shown in Figures 4 and 6. Likewise, high surface area 4:1 ITZ/EL100 particles (Figure 5) dissolved to a supersaturation of 12 within 10 min and precipitated to 5 after 1 h. For these high surface area particles, the excess surface areas were 0.11, 0.12, and 0.32 m^2, based on the supersaturation after 10 min (Table 1) resulting in rapid nucleation rates followed by growth that depleted the supersaturation within the first hour of dissolution. Similar behavior was observed for the high surface area 300 nm particles produced by salt flocculation of ITZ stabilized by HPMC and poloxamer 407, with a dose of 25.[39] As in the previous control experiment, the original nanoparticle dispersion was added dropwise to prevent buildup of excess particles and therefore the rapid decay in supersaturation. As a result, growth was inhibited yielding a supersaturation of 11 and 7.5 at 20 min and 2 h, respectively.[39] Otherwise, the use of particles with high surface areas was detrimental to maintaining long-term supersaturation due to the increased nucleation and growth from the increased excess undissolved surface area (Figure 1), despite the benefit of the initial rapid dissolution to produce a high maximum supersaturation. To further quantify the total extent of supersaturation over the 4 h experiment, the area under the curve (AUC) was calculated by numerical integration (Table 1).

4.3.3. Low Surface Area Particles. Low surface area 4:1 ITZ/HPMC SD and 4:1 ITZ/EL100 particles produced a minimal amount of excess surface area for a dose of 25 (Table 1). In the case of these slowly dissolving particles, the relatively low maximum supersaturation levels led to a low AUC, particularly for the HPMC case. The low excess surface area produced slow rates of growth from solution by condensation and coagulation, even for the relatively high supersaturation of 6 for 4:1 ITZ/EL100. This relatively stable and high supersaturation over 2 h indicates the advantage of electrostatic stabilizers to prevent growth while mitigating crystallization during dissolution. In addition as mentioned previously, the more rapid dissolution of EL100 versus HPMC may lead to a greater concentration of dissolved polymer chains to passivate growth of crystalline domains. Finally, the additional undissolved HPMC may act as nucleation sites for crystallization of the undissolved amorphous drug.

4.3.4. Medium Surface Area Particles. Medium surface area particles produced the highest AUC values in this work, particularly the salt flocculated particles in Figure 4. Despite the increase in the primary particle size of amorphous ITZ from ~500 nm to ~3 μm according to SEMs (Figure 2A−D), the dissolution was still sufficiently rapid to generate high supersaturation levels. In addition, the excess surface area of undissolved particles was sufficiently low to mitigate decay of supersaturation via nucleation and growth by condensation (Figure 1, eq A1) and coagulation (Figure 1, eq B1). For example, for the same starting AP dispersion containing a low polymer level, 4:1 ITZ/HPMC, the supersaturation was still 6 after 2 h for the salt flocculated sample versus only ~3 for the lyophilized sample with a corresponding AUC of 1869 versus 845 min.

On the basis of the similar peak supersaturations (Figure 4) alone, the driving force for nucleation and growth would have been similar for both lyophilized and salt flocculated particles. However, the lower excess surface area of the salt flocculated particles led to slower growth by condensation and coagulation, by 3.8 times. Thus, the medium surface area particles produced by salt flocculation offer an optimal balance of a sufficiently rapid dissolution rate, along with only moderate decay of supersaturation from a reduced excess surface area.

Recovery of particles by salt flocculation offers other advantages in addition to producing high supersaturation levels in pH 6.8 media. The particles may be recovered at 25 °C whereas relative temperatures >90 °C are necessary for spray drying. After salt flocculation, the dried particles have been shown to contain less than ~1% residual salt and the particles are more hydrophilic and more efficiently wetted by aqueous media than lyophilized powders, as is evident from smaller contact angles.[39] Finally the salt flocculation process produces higher yields and reduces the energy requirements relative to spray drying.[40]

4.3.5. Crystallinity of High and Medium Surface Area Particles. In this case, crystallinity of the final dried particles was not considered when comparing various particle specific surface areas. Partial crystallinity of the particles will lead to a decrease in the experimental supersaturation by decreasing the initial achievable supersaturation and acting as a sink to precipitate from the supersaturated solution.[52,53] Comparing the various particle formation techniques, the salt flocculated (medium surface area) particles were found to be the most crystalline followed by the AP lyophilized (high surface area) particles (Figure 3). In this case, the more crystalline medium surface area particles produced a higher sustained supersaturation resulting in a higher AUC. This unexpected result further confirms that an alternate mechanism is outweighing the expected decrease in achievable supersaturation based on the partial crystallinity of the particles.

4.4. Dissolution in pH 1.2 Media Followed by pH Shift to 6.8. To mimic the release of drug in the stomach followed by the transition to the upper intestine, selected

(52) Mosharraf, M.; Nystrom, C. Apparent Solubility of Drugs in Partially Crystalline Systems. *Drug Dev. Ind. Pharm.* **2003**, *29* (6), 603–622.

(53) Lindfors, L.; Skantze, P.; Skantze, U.; Westergren, J.; Olsson, U. Amorphous Drug Nanosuspensions. 3. Particle Dissolution and Crystal Growth. *Langmuir* **2007**, *23*, 9866–9874.

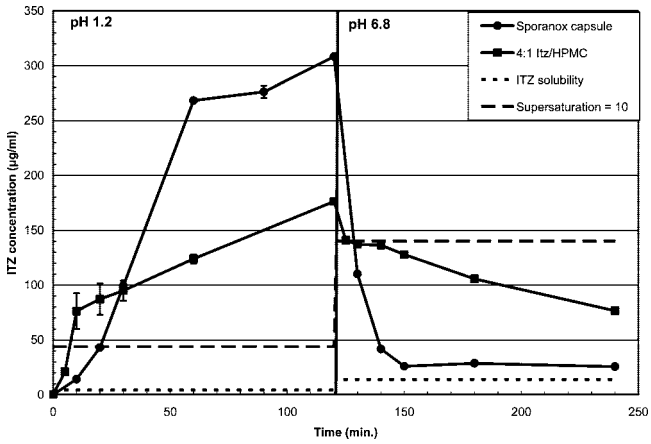

Figure 7. Supersaturation in pH 1.2 with a pH shift to 6.8 from dissolution of Sporanox capsule and 4:1 ITZ/HPMC at a dose of 350 μg/mL (based on pH 1.2 volume); equilibrium solubility of crystalline ITZ in pH 1.2 was 4.4 μg/mL and in pH 6.8 with 0.17% SDS was 14 μg/mL.

formulations were dissolved in pH 1.2 media for 2 h after which the pH was shifted to 6.8. The goal was to investigate how the quantity of dissolved drug at pH 1.2 affects the supersaturation behavior upon shifting to pH 6.8. The equilibrium solubilities were 4.4 and 14 μg/mL in the acidic and neutral media, respectively. The latter would have been only ~1 ng/mL,[54] in buffer without the addition of 0.17% SDS. Lyophilized AP 4:1 ITZ/HPMC was compared to the commercial solid ITZ product, Sporanox, which is a 20% (wt.) ITZ formulation including HPMC as a stabilizer.

As shown in Figure 7, high surface area lyophilized 4:1 ITZ/HPMC initially dissolved in pH 1.2 media yielded a supersaturation of ~12.5 and precipitated to only 5 even after 2 h at pH 6.8. When the same lyophilized 4:1 ITZ dose was added directly to pH 6.8 media, as shown in Figure 4, the supersaturation decayed more rapidly from 12 to 4 after only 20 min. Several factors contribute to the superior stability in supersaturation for the pH shift experiment. For example, approximately half of the mass dissolved at pH 1.2, which reduced the excess surface area available for precipitation from condensation and coagulation upon pH shift (see Table 1). Also, the HPMC had 2 h to dissolve in the acidic phase, therefore the amorphous drug was not trapped in a swollen slowly dissolving HPMC gel at pH 6.8, where it is likely to crystallize. Also the dissolved HPMC was then available to stabilize embryos which nucleated upon pH shift to 6.8, and slow down growth. Therefore, the dissolution of particles in pH 1.2 media to moderate supersaturation levels may reduce the depletion rate of supersaturation upon pH shift relative to direct dissolution in pH 6.8 media alone.

The dissolution of ITZ in Sporanox pellets in pH 1.2 media was rapid and almost complete within 2 h to produce a supersaturation of 70 (based on $C_{eq} = 4.4$ μg/mL at pH 1.2). Depletion to 40 μg/mL (supersaturation <3) occurred within 20 min after pH shift to pH 6.8, even though the shift in pH caused an increase in drug solubility from 4.4 to 14 μg/mL. The extremely high supersaturation appeared to produce fast nucleation rates and subsequent growth in pH 6.8 media, consistent with the rapid depletion of supersaturation from high specific surface area particles. As many nuclei were formed and grew, the dissolved HPMC was unable to adsorb to a sufficient level to protect against growth, as was evident by the rapid decay of supersaturation. From the results for the lyophilized 4:1 ITZ/HPMC particles, it is apparent that dissolution to moderate supersaturation levels under acidic conditions eliminates some excess surface area resulting is slower decay of supersaturation at pH 6.8.

5. Conclusions

Both high and medium surface area amorphous particles, recovered from aqueous dispersions of nanoparticles formed by antisolvent precipitation, rapidly dissolved in pH 6.8 media to generate supersaturation levels as high as 16 within 10 min. However, the decay in supersaturation was much slower for the medium relative to the high surface area particles. Lyophilization of the aqueous dispersions produced particles with high surface areas from 13 to 36 m^2/g. In contrast, salt flocculation of the particles in the aqueous dispersions followed by filtration produced ~3 μm particles with medium surface areas from 2 to 5 m^2/g. These particles were only partially crystallized despite the high degree of flocculation. By controlling the nature and composition of the polymer stabilizers on the surface, the particle size and surface area could be tuned over a wider range than in previous studies.[39,40] The relatively rapid dissolution of the high and medium surface area particles, before the undissolved particles crystallized, led to much higher maximum levels in supersaturation relative to more conventional low surface area (<1 m^2/g) solid dispersions. However, the slower nucleation and growth out of solution resulting from the lower excess surface area of undissolved medium surface area versus high surface area particles leads to higher AUCs. Thus, the medium surface area particles offer an optimum balance between favorable rapid dissolution and unfavorable nucleation and growth out of solution. A slow decay in supersaturation was also achieved by initially dissolving part of the drug at pH 1.2 to reduce the excess surface area of undissolved particles and then shifting the pH to 6.8.

Acknowledgment. We gratefully acknowledge the financial support from The Dow Chemical Company (Midland, MI). This material is based upon work supported in part by the STC Program of the National Science Foundation under Agreement No. CHE-9876674 and the Welch Foundation.

MP800106A

(54) Brewster, M. E.; Neeskens, P.; Peeters, J. Solubilization of itraconazole as a function of cyclodextrin structural space. *J. Inclusion Phenom. Macrocycl. Chem.* **2007**, *57*, 561–566.